IOPscience iopscience.iop.org

Home Search Collections Journals About Contact us My IOPscience

Magnetic Compton study of a USe single crystal

This article has been downloaded from IOPscience. Please scroll down to see the full text article.

1998 J. Phys.: Condens. Matter 10 6333

(http://iopscience.iop.org/0953-8984/10/28/014)

View the table of contents for this issue, or go to the journal homepage for more

Download details:
IP Address: 171.66.16.209
The article was downloaded on 14/05/2010 at 16:36

Please note that terms and conditions apply.

J. Phys.: Condens. Matter **10** (1998) 6333–6345. Printed in the UK PII: S0953-8984(98)89252-7

Magnetic Compton study of a USe single crystal

Hideo Hashimoto†, Hiroshi Sakurai†, Hiromi Oike†, Fumitake Itoh†, Akira Ochiai‡, Hidekazu Aoki§ and Takashi Suzuki§

† Department of Electronic Engineering, Faculty of Engineering, Gunma University, Kiryu, Gunma 376-8515, Japan

‡ Department of Material Science and Technology, Faculty of Engineering, Niigata University, Niigata, Niigata 950-2102, Japan

§ Physics Department, Graduate School of Science, Tohoku University, Sendai, Miyagi 980-0845, Japan

Received 14 November 1997, in final form 31 March 1998

Abstract. Magnetic Compton scattering experiments on a USe single crystal have been performed at several temperatures around the Curie temperature of the specimen. The spin and the orbital moments of USe are deduced by combining the magnetic Compton scattering experiment with the magnetization measurement. Furthermore, the spin moment of USe is decomposed into a 5f electron component and a diffused component. We have obtained the spin moment of the 5f electron $\mu_S(5f) = -1.09\ \mu_B$, the orbital moment of the 5f electron $\mu_L(5f) = 3.19\ \mu_B$ and the diffused moment $\mu_S(\text{diff}) = -0.31\ \mu_B$. From comparison with the previous results of UTe, it is concluded that the increase of the total magnetization from USe to UTe can mainly be ascribed to the decrease in magnitude of spin moment of the 5f electron with a slight increase of the orbital moment of the 5f electron. The results are also discussed from the points of view on the hybridization between U 5f and U 6d electrons and/or U 5f electrons and valence electrons of chalcogenide.

1. Introduction

Recently, much attention has been paid to the magnetic and electronic properties of actinide compounds from both theoretical and experimental sides. From these investigations, the behaviour of 5f valence electrons which characterize the magnetic and electronic properties of actinide compounds has been understood to be intermediate between 3d valence electrons of the transition metal systems and 4f valence electrons of rare-earth systems. In the case of transition metal systems, their magnetic properties are mainly dominated by 'itinerant' 3d valence electrons, which are well described by the energy band calculations. Since the crystal-field interaction is stronger than the spin–orbit interaction, the orbital moment, μ_L, is quenched and their magnetic moments are dominated by the spin moments, μ_S. On the other hand, in the case of rare-earth systems, their magnetic properties are mainly dominated by 'localized' 4f valence electrons, which are well described by the Heisenberg exchange model. Since the spin–orbit interaction is much stronger than the crystal-field interaction, the total angular momentum number, J, is a good quantum number and the orbital momentum and the spin momentum are expressed as $\mu_L = (2-g)J$ and $\mu_S = (2g-2)J$, respectively, where g is the Landé g factor [1, 2].

0953-8984/98/286333+13$19.50 © 1998 IOP Publishing Ltd

5f valence electrons of actinide compounds, however, are neither completely described in terms of the 'itinerant' model nor the 'localized' model. One of the reasons may be that the magnitude of spin–orbit interaction is comparable to that of crystal-field interaction. From this point of view, uranium monochalcogenides UX (X = S, Se and Te) have been extensively studied [2, 3]. The crystal structure of UX has the NaCl type and the lattice constant increases with increasing the atomic number of chalcogenide element. The UX undergoes a phase transition to a ferromagnetic state at 180, 160 and 104 K for X = S, Se and Te, respectively. The values of saturated magnetization of UX along the ⟨111⟩ direction as the easy-magnetization axis are 1.55, 1.82 and 1.91 μ_B, for X = S, Se and Te, respectively [3]. The decrease of Curie temperature and the increase of saturated moment correspond well to the increase of lattice constant, suggesting that the larger U–U spacing gives more localized 5f electrons of the U atom. The tendency of localization of 5f electrons against the atomic number of chalcogenide element has been supported by low temperature specific heat measurements [4]. However, the polar Kerr rotation angle shows the maximum in USe (2.6, 3.3, 3.1° for US, USe and UTe, respectively) [5, 6]. The decrease of the magneto-optical effect in UTe may point to a partial quenching of the orbital moment due to a substantial decrease of the spin–orbit interaction which can be attributed to strong f–d hybridization [7, 8]. Such a strong f–d hybridization has been also reported by several photoemission experiments [9–11].

Therefore, it would be essential to separate magnetic moment into the spin and orbital component in order to study the 5f magnetism in the uranium monochalcogenide compounds.

The magnetic Compton scattering experiment is inelastic scattering of x-rays [12]. The normal Compton profile, $J(p_z)$, is generally defined as the projection of the electron moment density, $n(\boldsymbol{p})$, along the scattering vector $\boldsymbol{K}$ which is conventionally defined as the z-direction,

$$J(p_z) = \iint n(\boldsymbol{p})\,\mathrm{d}p_x\,\mathrm{d}p_y. \tag{1}$$

The electron momentum p_z is given by the following equation

$$p_z = mc\frac{E_2 - E_1 + (E_1E_2/mc^2)(1-\cos\theta)}{\sqrt{E_1^2 + E_2^2 - 2E_1E_2\cos\theta}} \tag{2}$$

where E_1 and E_2 are the incident and the scattered x-ray energies, respectively, θ is the scattering angle, m is the electron mass, and c is the velocity of light. When polarized photons are used, the scattering cross section can be written as [13]

$$\frac{\mathrm{d}^2\sigma}{\mathrm{d}\Omega\,\mathrm{d}E_2} = r_0^2\frac{m}{2\hbar K}\left(\frac{E_2}{E_1}\right)\left[f_1J(p_z) + f_2\frac{E_1}{mc^2}P_cS(\alpha)J_{mag}(p_z)\right] \tag{3}$$

where

$$f_1 = 1 + \cos^2\theta + \frac{E_1 - E_2}{mc^2}(1-\cos\theta) + P_l\sin^2\theta \tag{4}$$

$$f_2 = -(1-\cos\theta) \tag{5}$$

and

$$S(\alpha) = s\left(\cos\alpha\cos\theta + \frac{E_2}{E_1}\cos(\theta-\alpha)\right) \tag{6}$$

where r_0 is the classical electron radius, P_c and P_l are the degree of circular and linear polarization of the beam, respectively, and the quantity s is ±1 depending on the direction of the magnetic field. α is defined as the angle between the direction of the incident x-ray

and the scattering vector [14]. $J_{mag}(p_z)$ in the second term of (3) is called as the magnetic Compton profile (MCP) and defined as a projection of the momentum distribution of the unpaired spin electrons, i.e.,

$$J_{mag}(p_z) = \iint \{n^{\uparrow}(\boldsymbol{p}) - n^{\downarrow}(\boldsymbol{p})\}\,\mathrm{d}p_x\,\mathrm{d}p_y \tag{7}$$

where $n^{\uparrow}(\boldsymbol{p})$ and $n^{\downarrow}(\boldsymbol{p})$ are the minority and majority subbands, respectively [12]. $J_{mag}(p_z)$ is normalized so as to give the spin moment μ_S as follows,

$$\mu_S = \int J_{mag}(p_z)\,\mathrm{d}p_z. \tag{8}$$

From the study of α-dependence in (3), it has been confirmed that the MCP can reflect only spin moment [14]. This is one of the most prominent features of the magnetic Compton scattering technique [15, 16]. This feature gives us the possibility to obtain separately spin and orbital contribution to the magnetic moment by combining the MCP with another magnetic measurement, for example, the total magnetization [14]. There exists another important feature of the magnetic Compton scattering technique: that the momentum distributions of different groups of electrons (3d, 4f, 5f, conduction electrons, etc) have characteristically different shapes of the MCP; thus one can obtain site- or shell-selective magnetic information in some cases such as $HoFe_2$ [14], $DyFe_2$ and $ErFe_2$ [17], Gd [18] and UFe_2 [19].

In a previous paper, we have already carried out the magnetic Compton scattering measurement of UTe and decomposed the magnetic moment into the spin and the orbital moment [20]. In this paper, we report the MCP of USe and separate the magnetic moment into the orbital and spin contribution. Furthermore, the decomposition of the spin contribution of USe into the uranium 5f component and diffused component is discussed. A comparison of the MCP between USe and UTe is discussed from the viewpoints of the degree of 5f localization and also the hybridization effect between U 5f and U 6d electrons, and/or between U 5f and chalcogenide valence electrons.

2. Experiment

2.1. Sample preparation

Single crystals of USe with high purity were grown by the Bridgman method using a prereacted powder technique [21], starting from uranium metal of 99.95% purity and selenium of 99.999% at the Oarai Branch, Institute for Materials Research, Tohoku University. The obtained lattice constant of USe single crystal was 5.750 Å, which agreed with the previous values [22, 23]. The temperature dependence of electrical resistivity ρ ($\mu\Omega$ cm) is shown together with its derivative $\mathrm{d}\rho/\mathrm{d}T$ in figure 1. The residual resistivity ρ_0 was 100.4 $\mu\Omega$ cm and the resistivity at room temperature was 363.1 $\mu\Omega$ cm. The residual resistivity rate was 3.62, which is larger than the previous one [24]. The Curie temperature, T_c, was deduced from the peak position of $\mathrm{d}\rho/\mathrm{d}T$ to be 173 ± 1 K, consistent with the temperature dependence of magnetization. Figure 2 shows the magnetization curve of the present USe at the field of 0.5 T along the ⟨100⟩, ⟨110⟩ and ⟨111⟩ directions. The saturated moment along the ⟨111⟩ direction per uranium atom, M, was 1.79 μ_B. The discrepancy of the physical properties of USe between the present and the previous data may be due to the specimen purity.

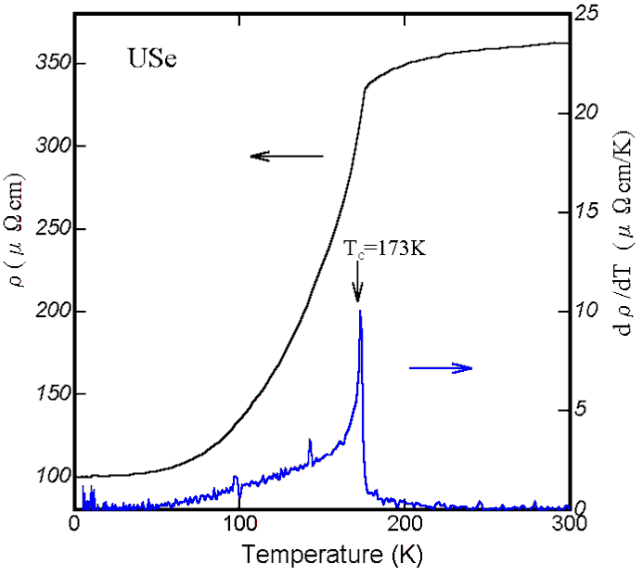

Figure 1. Temperature dependence of electrical resistivity $\rho(T)$ and the derivative $\mathrm{d}\rho/\mathrm{d}T$ of USe single crystal.

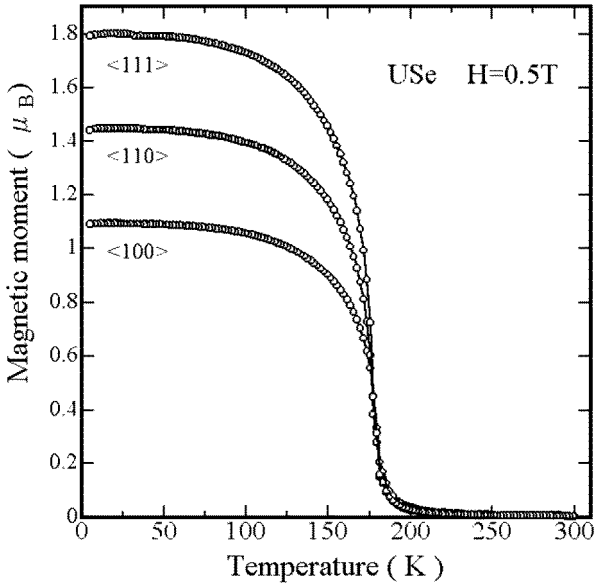

Figure 2. Temperature dependence of magnetization along ⟨100⟩, ⟨110⟩ and ⟨111⟩ directions of USe single crystal by SQUID under the magnetic field of $H = 0.5$ T.

2.2. Magnetic Compton scattering experiment

The single crystal of USe was cloven along the (100) plane of the crystal and shaped into a rectangle, 5.5 mm × 3 mm, with 1.5 mm thickness. The specimen was fixed on a Cu

disc sample holder with radius of 12 mm and was sealed by a Kapton foil with 12.5 μm thickness under 1 atmosphere of He gas to avoid the leakage of the nuclear fuel substance into the environment. The sample holder was then mounted on the top of the cold finger of the cryogenic refrigerator. The magnetic Compton scattering experiments were carried out at the NE-1 beam line of the accumulation ring in the National Laboratory for High Energy Physics (KEK). The experimental setup of this experiment is shown in figure 3. The circularly polarized incident x-rays emitted from the elliptical multipole wiggler were monochromatized by a doubly bent Si(111) monochromator [25], and then impinged onto the sample. The scattered x-rays were detected with 13-segmented solid state detectors (SSDs) of Ge located about 90 cm away from the sample. The average scattering angle of θ was $160^\circ \pm 2^\circ$. In this experiment, α in equations (3) and (6) was set to be $10^\circ \pm 2^\circ$. The resolution of each detector was 0.75 au (FWHM) in the momentum space. The counting rate for each detector was modulated so as to be below 20 000 (counts s^{-1}) at the initial ring current of 25–35 mA to avoid pile-up in the detector. The magnetic field of 0.5 T generated by an electromagnet was applied parallel or antiparallel to the direction of the scattering vector. It is to be noticed that the $\langle 100 \rangle$ direction of the sample makes an angle of $\phi = 15^\circ$ from the scattering vector $\boldsymbol{K}$ as shown in figure 3(b). The magnetic field was reversed in the sequence of $(+, -, -, +)$ with 15 second dwelling time where $+$ $(-)$ indicates the parallel (antiparallel) direction of the magnetization relative to the scattering

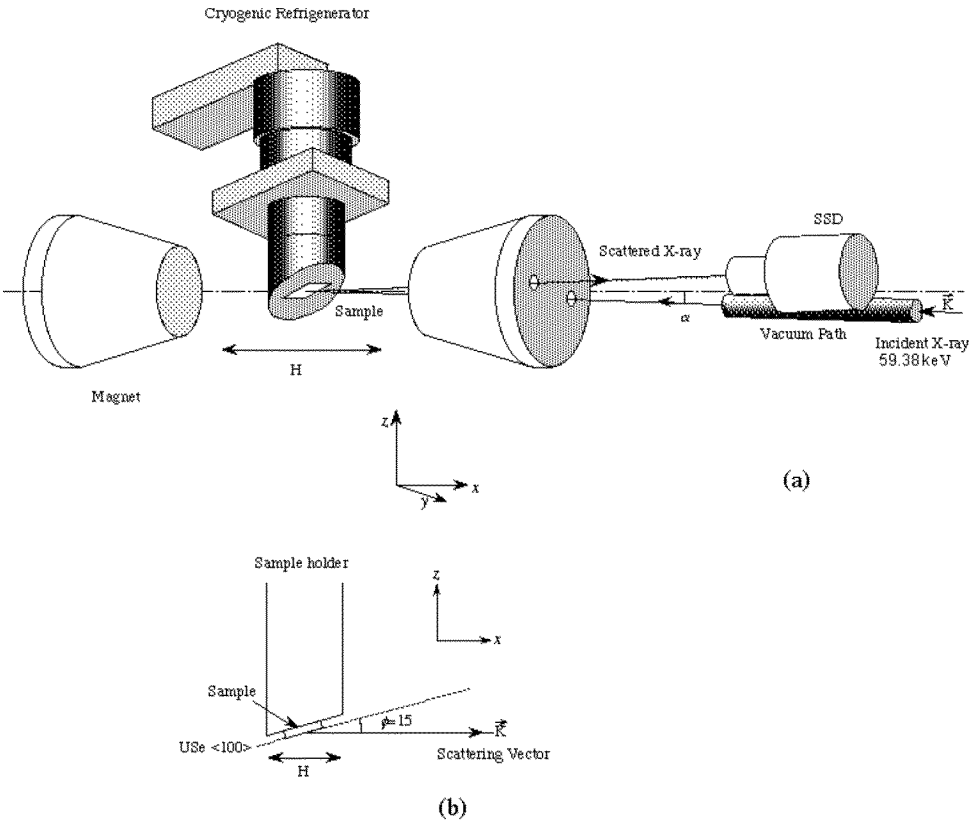

Figure 3. Experimental setup of magnetic Compton scattering experiment: (a) whole view with the scattering vector $\boldsymbol{K}$ in the x–y-plane; (b) side view of sample holder.

vector. The energy of the elliptically polarized incident beam (with the degree of circular polarization $P_c = 0.6$) was chosen to be 59.38 keV which is below the K edge of the uranium atom. The experiments were carried out at temperatures of 120, 150, 170, 190 and 210 K.

3. Experimental results

A spectrum of magnetic Compton scattered x-rays, $I_+ - I_-$, of USe at 150 K is shown in figure 4 as an example together with a reference spectrum of Fe at room temperature. I_+ (I_-) is the intensity of Compton scattered x-rays when the magnetic field was applied parallel (antiparallel) to the scattering vector direction. Figure 4 clearly shows that the sign of $I_+ - I_-$ of USe is opposite to that of Fe. This is a clear indication that the spin moment of USe is antiparallel to the magnetic field in contrast to the fact that the spin moment of Fe, i.e. 3d electrons, is parallel to the magnetic field. The feature has been already observed in the MCP measurements of UTe [20] and UFe_2 [19].

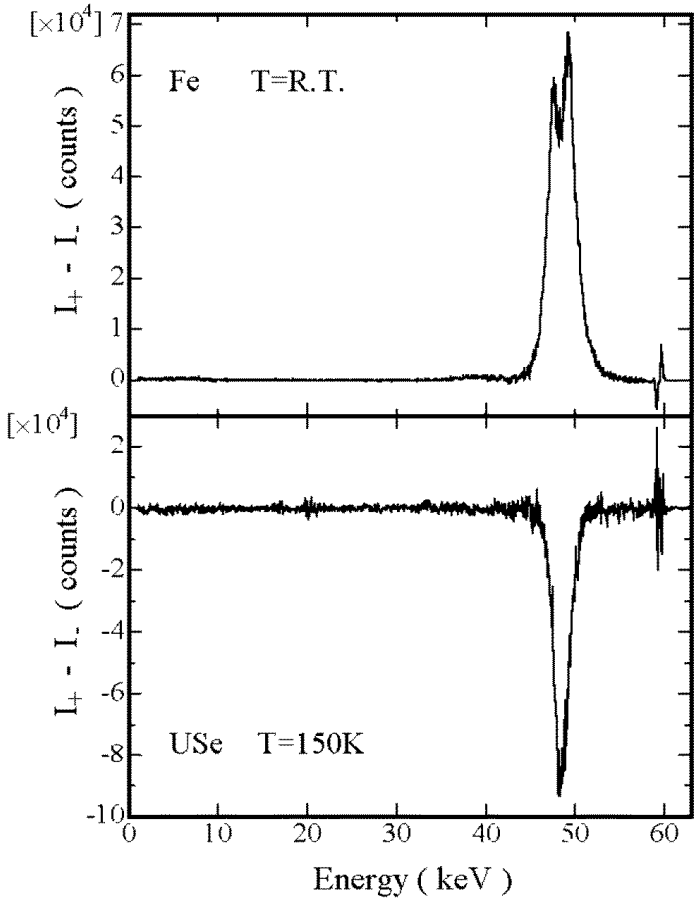

Figure 4. Spectra of magnetic Compton scattered x-rays, $I_+ - I_-$, of USe at 150 K together with Fe at room temperature for reference. Here, I_+ and I_- are intensities of Compton scattered x-rays for spin up (+) and spin down (−), respectively.

Firstly, we try to evaluate the spin moment value of USe. The flipping ratio R is defined as follows,

$$R = \frac{S_+ - S_-}{S_+ + S_-} \tag{9}$$

where S_+ (S_-) is the integrated intensity of I_+ (I_-). The spin moment of USe, μ_S(USe), is given by the following equation [20],

$$\mu_S(\mathrm{USe}) = \mu_S(\mathrm{Fe}) \left(\frac{A_{USe}}{A_{Fe}}\right) \left(\frac{R_{USe}}{R_{Fe}}\right). \tag{10}$$

Here, A is the number of electrons which take part in the Compton scattering event. Using the experimental values of $\mu_S(\mathrm{Fe}) = 2.219\ \mu_B$, $R_{\mathrm{Fe}} = 1.08 \times 10^{-2}$, $R_{\mathrm{USe}} = -8.28 \times 10^{-4}$, $A_{\mathrm{Fe}} = 26$ and $A_{\mathrm{USe}} = 126 - 2$ where the factor -2 comes from the fact that 1s electrons of U cannot take part in the present Compton scattering condition, the value of $\mu_S(\mathrm{USe}) = -0.81\ \mu_B$ was obtained as the spin moment of USe at 150 K (figure 2).

Two corrections are needed in order to estimate the saturated value of μ_S(USe) along the direction of $\langle 111 \rangle$. One is a factor which comes from the fact that the direction of applied magnetic field makes an angle β from the easy magnetization direction of $\langle 111 \rangle$. This factor was $\cos\beta$, where β was 45° from a simple calculation in the present set-up (figure 3). The other is a factor which comes from the reduction of saturated moment due to the temperature dependence as shown in figure 2. This factor was 0.81 at 150 K. After making these two corrections, we finally obtained $\mu_S(\mathrm{USe}) = -1.40 \pm 0.03\ \mu_B$ as the saturated spin moment of USe along the $\langle 111 \rangle$ direction.

Combining this saturated spin moment with the magnetization value, $M(\mathrm{USe}) = 1.79\ \mu_B$ from the magnetization measurement in this study, we obtain the orbital moment, μ_L(USe), as follows,

$$\mu_L(\mathrm{USe}) = M(\mathrm{USe}) - \mu_S(\mathrm{USe}) = 3.19 \pm 0.03\ \mu_B. \tag{11}$$

The temperature dependence of μ_S and μ_L thus obtained at various temperatures is shown in figure 5. It is seen that both the spin moment μ_S and the orbital moment μ_L behave similarly as a function of temperature. This fact suggests a reflection of strong L–S coupling in this system.

4. Discussion

4.1. The analysis of the structure of magnetic moment in USe

After making the energy dependent corrections for absorption and Compton cross-section in momentum space [26], the final magnetic Compton profile, $J_{mag}(p_z)$, of USe is shown in figure 6, where the integrated value of $J_{mag}(p_z)$ is normalized to give the spin moment of $-1.40\ \mu_B$. $J^{5f}_{mag}(p_z)$ in figure 6 denotes a Dirac–Hartree–Fock Compton profile of the uranium 5f electron [27] fitted to the experimental MCP by the least squares method in the high momentum region. The difference $J^{diff}_{mag}(p_z) = J_{mag}(p_z) - J^{5f}_{mag}(p_z)$ denoted by the crosses ($\times$) is ascribed to spin polarized conductive electrons, which we call the diffused component. It is interesting to note that the diffused component can be well fitted with a Compton profile of the uranium 6d wavefunction, $J^{6d}_{mag}(p_z)$. This implies that the diffused component is mainly dominated by the uranium 6d electron. From the above analysis, the total spin moment of USe, $\mu_S(\mathrm{USe}) = -1.40 \pm 0.03\ \mu_B$, is decomposed into 5f spin moment, $\mu_S(\mathrm{5f}) = -1.09 \pm 0.02\ \mu_B$, and diffused spin moment, $\mu_S(\mathrm{diff}) = -0.31 \pm 0.01\ \mu_B$

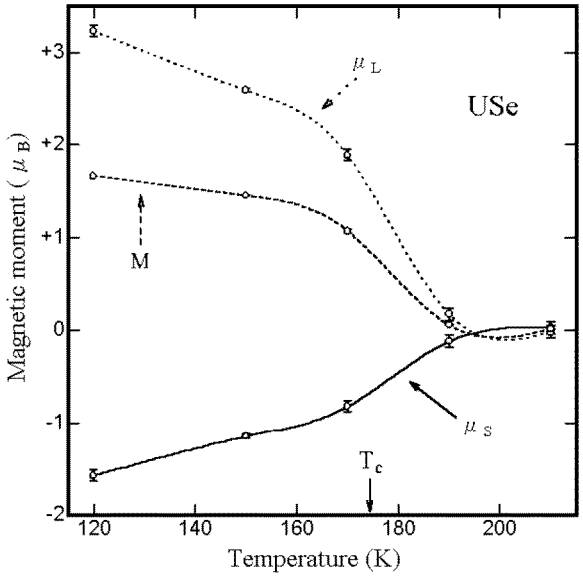

Figure 5. Temperature dependence of spin moment μ_S, orbital moment μ_L and total magnetization M in USe.

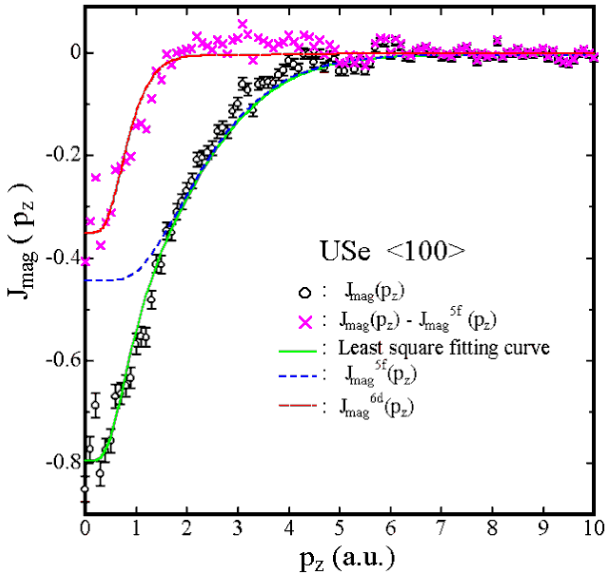

Figure 6. The magnetic Compton profile of USe, $J_{mag}(p_z)$. Theoretical calculations of the magnetic Compton profile of 5f component, $J_{mag}^{5f}(p_z)$, and 6d component, $J_{mag}^{6d}(p_z)$, are shown for comparison.

from the integration of $J_{mag}^{5f}(p_z)$ and $J_{mag}^{diff}(p_z)$ in figure 6. The negative signs of μ_S(5f) and μ_S(diff) mean that the spin moments of 5f electrons and the diffused moments are ferromagnetically coupled but align in the opposite direction to the magnetic field. This fact is consistent with the spin polarization measurement of the photoelectrons [11].

It would be reasonable to assume that the orbital moment of USe comes from mainly 5f electrons of uranium, that is to say, $\mu_L(\mathrm{USe}) = \mu_L(5\mathrm{f})$. Then, the total magnetic moment of 5f electrons of USe, $\mu_{total}(5\mathrm{f})$, can be deduced as follows,

$$\mu_{total}(5\mathrm{f}) \equiv \mu_L(5\mathrm{f}+) + \mu_S(5\mathrm{f}) = 2.10 \pm 0.04\ \mu_B. \tag{12}$$

Table 1. Magnetic moments of USe and UTe obtained from MCP study in Bohr units (μ_B). The values of magnetic moment from neutron scattering measurement and magnetization measurement are shown in parathesis [27] for comparison.

X	M(X)	μ_S(X)	μ_S(5f)	μ_S(diff)	μ_L(5f)	μ_{total}(5f)	$\mu_L(5\mathrm{f})/\mu_S(5\mathrm{f})$
USe	1.79	-1.40 ± 0.03	-1.09 ± 0.02	-0.31 ± 0.01	3.19 ± 0.03	2.10 ± 0.04	-2.92
	(1.82)			(-0.18)		(2.10 ± 0.10)	
UTe	1.87	-1.34[a]	-1.01	-0.33	3.22	2.20	-3.17
	(1.91 ± 0.05)			(-0.34)		(2.25 ± 0.05)	

[a] The magnetic moments of UTe have been reanalysed in the same way as that of USe described in the present text, therefore the numerical values have been corrected from the literature values [20].

The values of each component of the magnetization of USe are summarized in table 1 together with those of UTe. The corresponding values of magnetic neutron scattering experiment [28] are also referred in parenthesis for comparison. Table 1 shows that the total magnetic moment of 5f electrons, $\mu_{total}(5\mathrm{f})$, and the diffused spin moment, $\mu_S(\mathrm{diff})$, almost agree with those from neutron scattering experiments except for the $\mu_S(\mathrm{diff})$ in USe. The reason why there is some discrepancy in $\mu_S(\mathrm{diff})$ of USe between MCP and magnetic neutron experiment is unknown at the moment.

4.2. Comparison between USe and UTe in MCP

Now, we would like to compare the difference of MCP results between USe and UTe, focusing on the effects of the atomic number of the chalcogenide element. According to table 1, the total magnetic moment of 5f electrons, $\mu_{total}(5\mathrm{f})$, increases from USe to UTe in accordance with the saturated magnetization. This result shows qualitatively that the degree of localization of 5f electrons increases with increasing atomic number of chalcogenide element. However, table 1 shows that the spin contribution, $\mu_S(5\mathrm{f})$, and the orbital contribution, $\mu_L(5\mathrm{f})$, behave differently in the direction of change against the atomic number of chalcogenide element; the absolute value of 5f spin moment, $|\mu_S(5\mathrm{f})|$, decreases from 1.09 to 1.01 μ_B while the orbital moment of 5f electrons, $\mu_L(5\mathrm{f})$, slightly increases from 3.19 to 3.22 μ_B when one goes down from USe to UTe on the periodic table. The absolute value of diffused spin moment, $|\mu_S(\mathrm{diff})|$, also increases from 0.31 μ_B (USe) to 0.33 μ_B (UTe). Magnetic neutron experiments have also shown the same tendency as the present MCP experiment; the increase of conduction electron polarization with increasing atomic number of chalcogenide element [28]. The increase of $|\mu_S(\mathrm{diff})|$ from USe to UTe may come from the decrease of spin–orbit interaction due to stronger f–d hybridization [24] in UTe.

In order to understand more clearly the chalcogenide effects, the difference of MCP between USe and UTe is shown in figure 7 after normalizing each profile to the same area. The dashed curve in figure 7 is a theoretical curve which has been fitted with U 5f and U 6d Compton profiles as shown in figure 6. It is seen that the agreement between the experiment and the theory is rather poor. One of this discrepancy can come from the neglect of contribution from chalcogenide elements. This possibility of chalcogenide effect on MCP

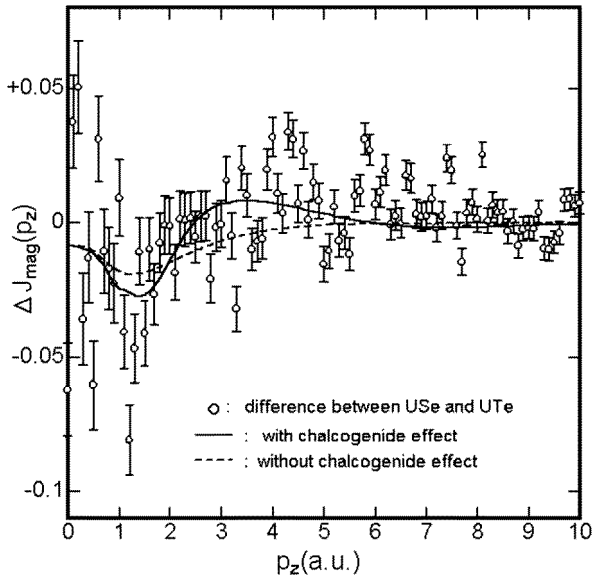

Figure 7. Difference of normalized magnetic Compton profile between USe and UTe, $\Delta J_{mag}(p_z) = J_{mag}^{USe}(p_z) - J_{mag}^{UTe}(p_z)$. Dashed curve is calculation fitted by two parameters (U 5f, 6d) and solid curve by six parameters (U 5f, 6d and Se 4s, 4p and Te 5s, 5p).

has been also suggested by the successful observation of x-ray magnetic circular dichroism at the L edges of Te in UTe [29]. The solid curve in figure 7 denotes another theoretical curve which takes into consideration of Compton profiles of Se(4s, 4p) and Te(5s, 5p) atomic wavefunctions in addition to those of U 5f and U 6d wavefunctions. The latter curve clearly gives better agreement with the experiment. This fact suggests that the hybridization between U 5f electrons and valence electrons of chalcogenides should be also taken into account in the analysis of the momentum distribution of uranium chalcogenides.

4.3. Hund's coupling model and intermediate coupling model

Hund's coupling model works as a good starting model of localized picture of 5f electrons to understand the physical picture of these materials. The orbital moment and spin moment have been deduced based on this model [20]. Table 2 shows calculated values of μ_L and μ_S for various 5f electron configurations of uranium based on a Hund's model in both USe and UTe using Landé g factor and the total angular momentum number J. In table 2, 5f total moment μ_{total}(5f) has been rescaled to the value obtained from MCP study. This rescaling would be allowed under the assumption that a weak crystal field only affects the magnetic moment by a constant factor without changing the relative ratio of the component in the magnetic moment [30]. The comparison of μ_S(5f), μ_L(5f) and the ratio μ_L/μ_S between table 1 and table 2 suggests that the 5f configuration of USe is between $f^2(U^{4+})$ and $f^3(U^{3+})$ but that the 5f configuration of UTe is between $f^1(U^{5+})$ and $f^2(U^{4+})$.

However, there are the strong 5f spin–orbit interaction and the 5f–5f Coulomb interactions in USe and UTe. These interactions may mix other LSJ levels into the Hund's rule ground state. Therefore, the intermediate coupling scheme would be more realistic for the estimation of each moment [30, 31]. The values estimated for USe and UTe from a intermediate coupling model of Collins *et al* [30] are shown in table 3. The

Table 2. The orbital moment μ_L, spin moment μ_S and the ratio μ_L/μ_S for various 5f configurations based on Hund's model. Each moment is rescaled so as to reproduce the 5f total moment value obtained from the MCP study.

	Uranium				USe			UTe			
	L	S	J	g_J	μ_L(5f)	μ_S(5f)	μ_{total}(5f)	μ_L(5f)	μ_S(5f)	μ_{total}(5f)	μ_L/μ_S
$f^1(U^{5+})$	3	$\frac{1}{2}$	$\frac{5}{2}$	$\frac{6}{7}$	2.79	−0.69	2.10	2.93	−0.73	2.20	−4.03
$f^2(U^{4+})$	5	1	4	$\frac{4}{5}$	3.15	−1.05	2.10	3.30	−1.10	2.20	−3.00
$f^3(U^{3+})$	6	$\frac{3}{2}$	$\frac{9}{2}$	$\frac{8}{11}$	3.67	−1.57	2.10	3.84	−1.64	2.20	−2.34
$f^3(U^{2+})$	6	2	4	$\frac{3}{5}$	4.89	−2.79	2.10	5.13	−2.93	2.20	−1.75

Table 3. The orbital moment μ_L, spin moment μ_S and the ratio μ_L/μ_S for various 5f configurations based on the intermediate coupling model taken from Collins *et al* [30]. Each moment is rescaled so as to reproduce the 5f total moment value obtained from the MCP study.

	USe			UTe			
	μ_L(5f)	μ_S(5f)	μ_{total}(5f)	μ_L(5f)	μ_S(5f)	μ_{total}(5f)	μ_L/μ_S
$f^1(U^{5+})$	3.20	−1.08	2.10	3.35	−1.12	2.20	−2.97
$f^2(U^{4+})$	2.98	−0.88	2.20	3.11	−0.92	2.20	−3.38
$f^3(U^{3+})$	3.46	−1.36	2.10	3.62	−1.42	2.20	−2.55
$f^4(U^{2+})$	4.56	−2.46	2.10	4.77	−2.57	2.20	−1.85

comparison of μ_S(5f), μ_L(5f) and the ratio μ_L/μ_S between table 1 and table 3 suggests that 5f configurations of both USe and UTe are between $f^2(U^{4+})$ and $f^3(U^{3+})$. This fact qualitatively agrees with the 5f configuration from photo-emission experiment [10] and the number of f electrons, 2.68 in UTe, from the band structure calculation [32].

As a consequence, the intermediate coupling model seems to be more realistic than the rescaled Hund's model for describing uranium 5f configurations of USe and UTe under this investigation. Therefore, these results suggest that the ground states of USe and UTe are expected to be mainly a mixture of $f^2(U^{4+})$ and $f^3(U^{3+})$ configurations.

5. Conclusion

The MCP measurements have been performed on a high quality single crystal of USe at temperatures of 120, 150, 170, 190 and 210 K. Obtained results are summarized as follows.

(1) Combining the MCP measurements with the magnetization measurements, the spin and the orbital contribution of USe have been separated. The spin moment μ_S (orbital moment μ_L) is found to be aligned antiparallel (parallel) to the magnetic field. Also, the separated spin and the orbital contributions give similar temperature dependence to the total magnetization within experimental errors.

(2) The MCP of USe has been decomposed into two components; one is the 5f spin component, μ_S(5f), which is rather localized, and the other is the diffused component, μ_S(diff), which is rather itinerant. The total 5f moment, $\mu_{total}(5f) = \mu_S(5f) + \mu_L(5f)$, has been obtained in good agreement with the neutron experiment.

(3) A comparison of L/S separation between USe and UTe in the MCP study has resulted into the decrease of $|\mu_S(5f)|$, and the increase of both $|\mu_S(\text{diff})|$ and μ_L(5f). The

increase of the magnetization M from USe to UTe is confirmed by the increase of total 5f moment μ_{total}(5f), and it is mainly due to the decrease of $|\mu_S(5f)|$ since the quantity of change in both $|\mu_S(\text{diff})|$ and $\mu_L(5f)$ between USe and UTe is small. This behaviour can be ascribed to the decrease of the spin–orbit interaction associated with the hybridization between U 5f electrons and U 6d electrons and/or between U 5f electrons and valence electrons of chalcogenide elements. The stronger hybridization in UTe compared to USe is reflected by the observation of the MCP difference between USe and UTe.

(4) Concerning the uranium 5f configurations, the intermediate coupling model gives a more realistic picture than the rescaled Hund's model, which suggests that the 5f configurations for both USe and UTe lie between $5f^2$ and $5f^3$.

In order to understand more quantitatively the uranium 5f state, theoretical calculation is highly required which takes into account the effect of interactions between uranium and chalcogenide elements.

Acknowledgments

The present authors would like to express great thanks to Mr Y Suzuki at the Oarai Branch, Institute for Materials Research, Tohoku University for handling the uranium specimen for this experiment, and Professor H Kawata at the High Energy Accelerator Research Organization, Institute of Materials Structure Science, Photon Factory (KEK-PF) for his encouragement during this study. We also would like to express sincere thanks to the authorities of the KEK-PF for allowing us to use the nuclear fuel substances for the measurements under the proposal number 94G-532 and 96G-262. The authors also acknowledge that a part of this work has been done using the SQUID magnetometer at Venture Business Laboratory, Gunma University.

References

[1] Lander G H, Brooks M S S and Johansson B 1991 *Phys. Rev.* B **43** 13 672
[2] Brooks M S S, Johansson B and Skriver H L 1984 *Handbook on the Physics and Chemistry of the Actinides* vol 1, ed A J Freeman and G H Lander (Amsterdam: North-Holland) ch 3
[3] Vogt O 1980 *Physica* B **102** 206
[4] Rudigier H, Ott H R and Vogt O 1985 *Phys. Rev.* B **32** 4584
[5] Reim W 1986 *J. Magn. Magn. Mater.* **58** 1
[6] Schoenes J 1980 *Phys. Rep.* **66** 187
[7] Reim W, Schoenes J and Vogt O 1984 *J. Appl. Phys.* **55** 1853
[8] Lim S P, Price D L and Cooper B R 1991 *IEEE. Trans. Magn.* **MAG-27** 3648
[9] Reihl B, Mårtensson N and Vogt O 1982 *J. Appl. Phys.* **53** 2008
[10] Reihl B, Mårtensson N, Heimann P, Eastman D E and Vogt O 1981 *Phys. Rev. Lett.* **46** 1480
[11] Erbudak M, Greuter F, Meier F, Reihl B, Vogt O and Keller J 1979 *J. Appl. Phys.* **50** 2099
[12] Platzman P M and Tzoar N 1970 *Phys. Rev.* B **2** 3556
[13] Lipps F W and Tolhock H A 1954 *Physica* **20** 85
Lipps F W and Tolhock H A 1954 *Physica* **20** 395
[14] Cooper M J, Zukowski E, Timms D N, Armstrong R, Itoh F, Tanaka Y, Ito M, Kawata H and Bateson M 1993 *Phys. Rev. Lett.* **71** 1095
[15] Cooper M J, Zukowski E, Collins S P, Timms D N, Itoh F and Sakurai H 1992 *J. Phys.: Condens. Matter* **4** L399
[16] Sakai N 1994 *J. Phys. Soc. Japan* **63** 4655
[17] Lawson P K, McCarthy J E, Cooper M J, Laundy D, Collins S P, Itoh F, Sakurai H, Iwazumi T, Kawata H, Ito M, Sakai N and Tanaka Y 1995 *J. Phys.: Condens. Matter* **7** 389
[18] Sakai N, Tanaka Y, Itoh F, Sakurai H, Kawata H and Iwazumi T 1991 *J. Phys. Soc. Japan* **60** 120
[19] Lawson P K, Cooper M J and Dixon M A G 1997 *Phys. Rev.* B **56** 3239

[20] Sakurai H, Hashimoto H, Ochiai A, Suzuki T, Ito M and Itoh F 1995 *J. Phys.: Condens. Matter* **7** L599
[21] Ochiai A 1994 *Physica* B **199/200** 616
[22] Brooks M S S 1984 *J. Phys. F: Met. Phys.* **14** 653
[23] Wedgewood F A and Kuzniets Moshe 1972 *J. Phys. C: Solid State Phys.* **5** 3012
[24] Schoenes J, Frick B and Vogt O 1984 *Phys. Rev.* B **30** 6578
[25] Kawata H *et al* 1989 *Rev. Sci. Instrum.* **60** 1885
[26] Grotch H, Kazes E, Bhatt G and Owen D A 1983 *Phys. Rev.* A **27** 243
[27] Biggs F, Mendelsohn L B and Mann J B 1975 *At. Data Nucl. Data Table* **16** 201
[28] Buyers W J L and Holden T M 1985 *Handbook on the Physics and Chemistry of the Actinides* vol 2, ed A J Freeman and G H Lander (Amsterdam: North-Holland) ch 4
[29] Hashimoto H, Sakurai H, Oike H, Itoh F, Ochiai A, Aoki H and Suzuki T 1998 to be published
[30] Collins S P, Laundy D, Tang C C and van der Laan G 1995 *J. Phys.: Condens. Matter* **7** 9325
[31] Chen S-K and Lam D J 1974 *The Actinides: Electronic Structure and Related Properties* vol 1, ed A J Freeman and J B Darby (New York: Academic) ch 1
[32] Trygg J, Wills J M, Brooks M S S, Johansson B and Eriksson O 1995 *Phys. Rev.* B **52** 2496